

# Optimal Control for Sport Utility Vehicle System Using Linear Quadratic Integral Control Approach

M. F. Omar<sup>1</sup>, R. Ghazali<sup>1\*</sup>, I. M. Saadon<sup>2</sup>, M. K. Aripin<sup>1</sup>, Y. M. Sam<sup>3</sup> and C. C. Soon<sup>1</sup>

<sup>1</sup>*Center for Robotics and Industrial Automation, Faculty of Electrical Engineering, Universiti Teknikal Malaysia Melaka, 76100 Durian Tunggal, Melaka, Malaysia.*

<sup>2</sup>*Faculty of Engineering Technology, Universiti Teknikal Malaysia Melaka, 76100 Durian Tunggal, Melaka, Malaysia.*

<sup>3</sup>*School of Electrical Engineering, Universiti Teknologi Malaysia, 81310 Skudai, Johor, Malaysia*  
\*[rozaimi.ghazali@utem.edu.my](mailto:rozaimi.ghazali@utem.edu.my)

**Abstract**— The Sport Utility Vehicle (SUV) has become one of the popular vehicles to be chosen, since it was first introduced. However, the higher Centre of Gravity (C.G) and the bigger sizing at the side area have led to the stability and the handling issues that degrade the vehicle's performances, especially during the confrontation with external disturbances. This paper presents an analysis of an optimal control that enhances the handling and stability of the SUV. The Direct Yaw Control (DYC) method was used to control the vehicle's accuracy and robustness towards environmental parameters during the critical manoeuvre. The Linear Quadratic Regulator (LQR) and Linear Quadratic Integral (LQI) were compared to obtain the optimal performances during the control of the vehicle's handling and stability. With the interference of an external disturbance during the critical manoeuvre, the results indicate that the LQI produce significant improvement in the vehicle's handling and stability control.

**Index Terms**—Optimal Control; Direct Yaw Moment; SUV; LQI.

## I. INTRODUCTION

Vehicle dynamics play an important role in safety and stability during severe cornering and critical situation, especially for yaw rate and sideslip angle in a lateral motion. A report in [1] claimed that the usage of the Sport Utility Vehicle (SUV) has been increasing and become popular every year compared with passenger cars since the 1990s. However, the SUV vehicle leads to more accidents due to its higher Centre of Gravity (CG) and heavier than a normal sedan car as discussed in [2, 3]. Another drawback of SUV is the bigger size of side area where it can affect the stability of the vehicle when an external disturbance struck the vehicle such as sidewind as reported in [2]. The structural characteristic of the SUV may lead to unstable and undesirable vehicle movement, such as excessive understeer and oversteer in lateral motion during severe cornering or under critical situation.

To overcome these problems, researchers and engineers have proposed active-based system such as autonomous vehicle steering using Global Position System (GPS) in [4]. The study in [5], implemented Advance Driver Assistance System (ADAS) using warning system based on steering intervention strategy and another active system is Active Chassis System (ACS), also called as Electronic Stability Control (ESC), where the system directly controls the motion of the vehicle using available sensor and actively regulates the brake actuator. The ESC system can be divided

into several active chassis controls, namely Active Steering, Steer-By-Wire, Torque Vectoring System (TVC), Four Wheel Independent Drive (4WID) and Direct Yaw Control (DYC).

The DYC has been widely used for current ESC system, where the Anti-lock Braking System (ABS) is fully utilized by applying the differential braking at the left or right and front or rear wheel to control the yaw moment of the vehicle. The main benefit of using DYC is due to its control method that are strongly robust to the environment parameters and highly accurate during the control of the vehicle at the critical situation [6]. Since the introduction of the ESC system, numerous researchers have proposed various control techniques to improve the vehicle handling and safety of SUV. For example, [7] applied a nonlinear controller using Sliding Mode Controller (SMC) to enhance the differential braking of SUV and improve the interaction of the driver with controller. Studies in [8], proposed Model Predictive Control (MPC) with SMC controller to enhance the SUV handling by improving the slip ratio of four-wheel and overcome the nonlinearity with uncertainty of tire-road contact condition. An Artificial intelligent (A.I) controller is implemented in [9] using Fuzzy Logic Control (FLC) by integrating active roll control (ARC) with DYC to improve the handling of the SUV and in [10], a Self-Tuning Fuzzy Proportional-Integral-Proportional-Derivative (STFPI-PD) controller has been proposed to overcome the derivative kick problem.

Furthermore, many researchers have proposed a Linear Quadratic Regulator (LQR) based on optimal control theory as their control technique because this approach has the advantage of achieving stability in certain bandwidth, and satisfying number of properties as well as possesses a number of desirable constraints as demanded by the designer in their system [11]. The work done in [12] utilized the LQR controller at upper-level controller to achieve an optimum brake distribution torque and maximize the regenerative brake torque for fuel economy as well as prevent the front tire from saturation. Study in [13] proposed the Linear Quadratic Static Output Feedback (LQSOF) to overcome the parameter sensitivity using heuristic search of Covariance Matrix Adaptation-Evolutionary Computation (CMA-EC) to find the optimal gain, K. The electro hydraulic brake based on LQR method is used in [14] for multi-objective to improve the yaw rate and roll stability for SUV, while in [15] and [16], an investigation of the driver-in-the-loop real-simulations reconstructed by vehicle simulator using LQR controller has been done. But mostly,

the design based on LQR controller theory is not robust enough against uncertainties, external disturbance or un-modelled dynamic. According to [17], the integral action is used to eliminate the offset in system parameters of LQR and make the system to be more robust against measurement noise, external disturbances and un-modelled dynamics. In this paper, a comparison of LQR and LQI based on optimal control theory to investigate the effectiveness of these two controllers towards SUV parameter and external disturbances is proposed.

This paper is organized as follows. In Section II, the vehicle dynamic model is presented. The controllers design and structure are explained in Section III. In section IV, the computer simulation result with discussions is presented and finally, the final remark will be concluded in Section V.

## II. VEHICLE DYNAMIC MODEL

Figure 1 shows the schematic diagram of 3 Degrees of Freedom (DOF) nonlinear models that represent the vehicle handling dynamics of an SUV in a yaw plane, including the longitudinal motion, lateral motion, yaw motion and sideslip angle.

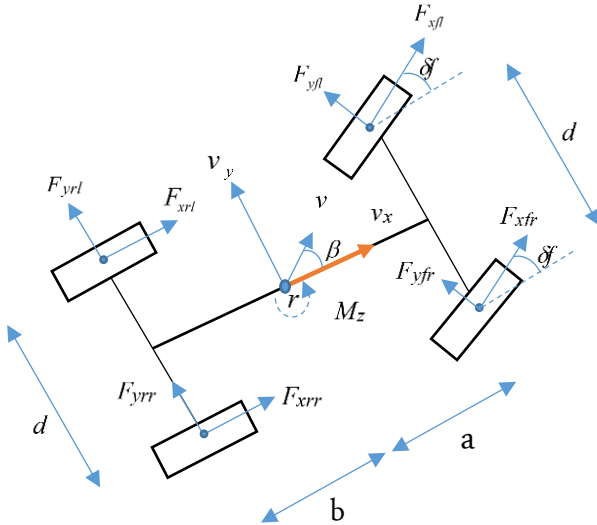


Figure 1: Nonlinear vehicle model

The front wheel steer angle represents an input denoted by  $\delta_f$ , while yaw rate,  $r$  and sideslip,  $\beta$  are the output variables need to be controlled. The vehicle parameters of  $a$  and  $b$  are the distance from the front and rear to the Centre of Gravity (C.G) respectively. The  $d$  is the vehicle width track and  $M_z$  is yaw moment. The  $v_y$  and  $v_x$  are lateral and longitudinal velocity respectively. Then, the longitudinal tires forces are donated as  $F_{xfl}$  for the front left tires,  $F_{xfr}$  for the front right tires,  $F_{xrl}$  for the rear left tires and the rear right tires is  $F_{xrr}$ . The lateral forces at the front left, front right, rear left and rear right tires are given by  $F_{yfl}$ ,  $F_{yfr}$ ,  $F_{yrl}$  and  $F_{yrr}$ , respectively. Other parameters that must be taken into account are cornering stiffness at the front and rear tire,  $C_f$  and  $C_r$ , vehicle mass  $m$ , and moment of inertia  $I_z$ .

The equation of longitudinal, lateral and yaw motions of vehicle body can be described as follows [18]:

$$\begin{aligned} m\dot{a}_x &= m(\dot{v}_x - rv_y) \\ &= (F_{xfl} + F_{xfr})\cos(\delta_f) + F_{xrl} + \dots \\ &\quad \dots + F_{xrr} - (F_{yfl} + F_{yfr})\sin(\delta_f) \end{aligned} \quad (1)$$

$$\begin{aligned} m\dot{a}_y &= m(\dot{v}_y + rv_x) \\ &= (F_{yfl} + F_{yfr})\cos(\delta_f) + F_{yrl} + \dots \\ &\quad \dots + F_{yrr} + (F_{xfl} + F_{xfr})\sin(\delta_f) \end{aligned} \quad (2)$$

$$\begin{aligned} I_z\dot{r} &= a(F_{xfl} + F_{xfr})\sin(\delta_f) + a(F_{yfl} + F_{yfr})\cos(\delta_f) \\ &\quad - b(F_{yrl} + F_{yrr}) + M_z \end{aligned} \quad (3)$$

The tires tend to turn at z-axis when the yaw moment is bigger than zero value. The yaw rate  $r$  and sideslip  $\beta$  can be determined by lateral acceleration,  $a_y$  in forward speed  $v$  as follows:

$$a_y = \dot{v}_y + rv_x = v(r + \dot{\beta}) \quad (4)$$

By using the two-track model as a reference, the equation from (3) can be expressed as follows:

$$\dot{r} = \frac{1}{I_z} \left[ a(F_{yfl}\cos\delta_f + F_{yfr}\cos\delta_f + F_{xfl}\sin\delta_f + F_{xfr}\sin\delta_f) - b(F_{yrl} + F_{yrr}) + M_z \right] \quad (5)$$

While the variable of sideslip  $\beta$  can be obtained as follows:

$$\dot{\beta} = \frac{1}{mv} \left[ \cos\beta(\cos\delta_f(F_{xfl} + F_{xfr}) - \sin\delta_f(F_{yfl} + F_{yfr})) - \sin\beta(\sin\delta_f(F_{xfl} + F_{xfr}) - \sin\delta_f(F_{yfl} + F_{yfr})) \right] - r. \quad (6)$$

Slip angle or sideslip angle is the angle between the actual travel of wheel rolling direction and the direction where the wheel is pointing. The sideslip angle at the front and rear tires are defined by the following equation:

$$\alpha_f = \delta - \frac{\dot{y} + a\dot{\psi}}{\dot{x}} \quad (7)$$

$$\alpha_r = -\frac{\dot{y} - b\dot{\psi}}{\dot{x}} \quad (8)$$

where,

$\dot{x}$  = Longitudinal velocity       $\dot{\psi}$  = Yaw rate  
 $\dot{y}$  = Lateral velocity       $\delta$  = Steering angle

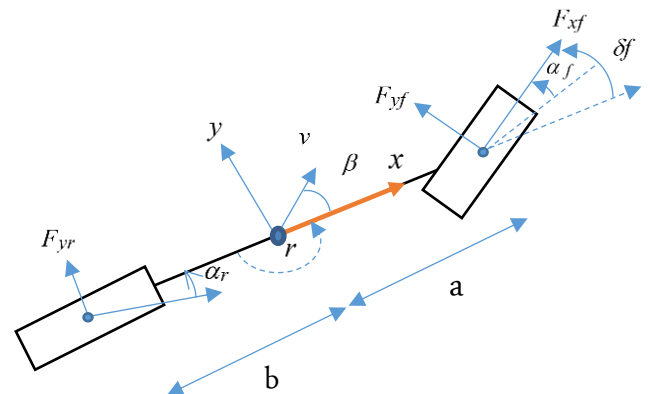


Figure 2: Bicycle Model

The 2 DOF or bicycle model in Figure 2 represents the desired model because it has the simplest form of planar

motion and it can only be used for analyzing the lateral and yaw motions. In the bicycle model, there are certain assumptions such as fixed/constants forward speed, tires forces that operate in the linear region, two front wheels that have the same steering angle, non shifted C.G as the vehicle mass is changing, small angle approximation and negligible self-alignment torque wheel. Further, the two wheels at the front and rear are combined and become one single unit and the width track is ignored. The configuration of the SUV is the front wheel drive and the wheel dynamics are negligible. The lateral and yaw motions can be described based on the following equations:

$$mv(\dot{\beta} + r) = (F_{yf} + F_{yr}) - r \quad (9)$$

$$I_z \dot{r} = a(F_{yf} - b)F_{yr} \quad (10)$$

The bicycle model indicated a linear characteristic. Therefore, by using the equations of (6) and (7), the cornering stiffness for the front and rear tires can be obtained by the following equations:

$$F_{yf} = C_f \alpha_f \quad (11)$$

$$F_{yr} = C_r \alpha_r \quad (12)$$

By using the linear state space model, the differential equation of variable yaw rate and sideslip can be obtained by rearranging and simplified the equation (7) to (12) as follows:

$$\dot{x} = Ax + Bu,$$

$$\begin{bmatrix} \dot{\beta} \\ \dot{r} \end{bmatrix} = \begin{bmatrix} a_{11} & a_{12} \\ a_{21} & a_{22} \end{bmatrix} \begin{bmatrix} \beta \\ r \end{bmatrix} + \begin{bmatrix} b_{11} & b_{12} \\ b_{21} & b_{22} \end{bmatrix} u, \quad (13)$$

where,

$$\begin{aligned} a_{11} &= \frac{C_f a - C_r b}{mv_x^2} - 1 & a_{12} &= \frac{C_f + C_r}{mv_x} \\ a_{21} &= \frac{C_f a^2 - C_r b^2}{I_z v} & a_{22} &= \frac{C_r b - C_f a}{I_z} \\ b_{11} &= \frac{C_f}{mv} & b_{12} &= 0 \\ b_{21} &= \frac{C_f a}{I_z} & b_{22} &= \frac{1}{I_z} \end{aligned}$$

By implementing the Laplace Transform, the following equation will be obtained:

$$(s - a_{11}) \cdot \beta(s) - a_{12} \cdot r(s) = b_{11} \cdot \delta(s) \quad (14)$$

$$-a_{21} \cdot \beta(s) + (s - a_{22}) \cdot r(s) = b_{22} \cdot M(s) + b_{21} \cdot \delta(s) \quad (15)$$

Then, the sideslip angle  $\beta(s)$  and yaw rate  $r(s)$  can be derived further [22] as below:

$$B(s) = \frac{(b_{11}s - a_{22}b_{11} + a_{12}b_{21})\delta + (a_{12}b_{22})M}{(s - a_{11})(s - a_{22}) - a_{12}a_{21}} \quad (16)$$

$$r(s) = \frac{(a_{21}b_{11} + b_{21}s + a_{11}b_{21})\delta_f(s) - (a_{11}b_{22} - b_{22}s)M(s)}{(s - a_{11})(s - a_{22}) - a_{12}a_{21}} \quad (17)$$

The design of feedforward compensation is to control the sideslip angle to become a zero value. Therefore, the relationship between the two control input, direct yaw moment,  $M(s)$  and front steering angle  $\delta_f(s)$  is assumed as below:

$$M(s) = P_{ff} \cdot \delta_f(s) \quad (18)$$

where  $P_{ff}$  is the proportional gain feedforward controller. By solving the equation (17) and (18), the result of the feedforward gain can be obtained as:

$$P_{ff} = \frac{b_{11} \cdot a_{22} - b_{21} \cdot a_{12}}{a_{12} \cdot b_{22}} \quad (19)$$

Further, by substituting the equation (19) and (18) into equation (17), the transfer function of yaw rate with respect to front steering angle will be obtained as follows:

$$\gamma(s) = \frac{b_{11} \cdot a_{22} \cdot s + (b_{11} \cdot a_{12} \cdot a_{21} - b_{11} \cdot a_{11} \cdot a_{22})}{a_{12} [s^2 - (a_{11} + a_{12})s + a_{11} \cdot a_{22} - a_{12} \cdot a_{21}]} \delta_{f0}(s) \quad (20)$$

As a desired vehicle model (2 DOF), the reference of yaw rate is modelled on the 1st order delay system by setting the  $\begin{bmatrix} \dot{\beta} \\ \dot{r} \end{bmatrix} = 0$  and solving the  $\gamma$  in (13) and for sideslip angle, the desired model is designed with a zero value at a steady state.

$$X_d = \begin{bmatrix} \beta_d \\ \gamma_d \end{bmatrix} = \begin{bmatrix} 0 \\ \frac{\gamma_{ssg}}{\tau_r s + 1} \end{bmatrix} \delta_f \quad (21)$$

where,

$\gamma_{ssg}$  = Steady state yaw rate gain

$\tau_r$  = Delay time constant

The steady state yaw rate gain can be obtained by comparing the equation (20) and (21), as follows:

$$\gamma_{ssg} = \frac{b_{11}(a_{12} \cdot a_{21} - a_{11} \cdot a_{22})}{a_{12}(a_{11} \cdot a_{22} - a_{12} \cdot a_{21})} \quad (22)$$

and the ideal vehicle model can be expressed in (23), as the following expression:

$$\dot{X}_d = A_d \cdot X_d + E_d \cdot \delta_f \quad (23)$$

### III. CONTROLLER DESIGN

In this work, the yaw rate and sideslip angle of SUV affect the handling and stability of the vehicle during critical manoeuvre and situation. By using DYC technique, the yaw rate and sideslip angles can be controlled to stabilize and ensure a proper response for SUV during the critical dynamic behaviour of the vehicle. The objective of the control system is to make the actual vehicle model follows the desired vehicle model by calculating the value of yaw rate,  $\gamma$  and follows the desired value of yaw rate,  $\gamma_d$ . The

purpose of controlling the sideslip angle is to prevent the vehicle from spinning or the wheel from being out of control from the pointed direction of the wheel. This condition can be achieved by limiting the sideslip angle,  $\beta$ . By using DYC technique, the yaw moment is generated by regulating the slip ratio of the wheel between the difference of the left and right tire longitudinal forces.

To design the feedback controller, the state equation (13) needs to be transformed into the expression below:

$$\begin{bmatrix} \dot{\beta} \\ \dot{\gamma} \end{bmatrix} = \begin{bmatrix} a_{11} & a_{12} \\ a_{21} & a_{22} \end{bmatrix} \begin{bmatrix} \beta \\ \gamma \end{bmatrix} + \begin{bmatrix} e_1 \\ e_2 \end{bmatrix} \delta_f + \begin{bmatrix} b_1 \\ b_2 \end{bmatrix} M \quad (24)$$

where,

$$e_1 = -\frac{C_f}{mv_x} \quad e_2 = -\frac{C_f l_f}{I_{zz}} \quad b_1 = 0 \quad b_2 = \frac{1}{I_{zz}}$$

Therefore, the new state equation is,

$$\dot{X} = A.X + B.M + E.\delta_f \quad (25)$$

By assuming the difference between the ideal model and the actual model as an error,  $e$  and by differentiating this error in (26), the expression becomes as (27):

$$e = X - X_d \quad (26)$$

$$\dot{e} = \dot{X} - \dot{X}_d \quad (27)$$

then the equations (23) and (25) are replaced into the equation (27) to derive equation (28). By simplifying equation (28), the following results will be obtained:

$$\dot{e} = A.X - A.X_d + A.X_d - A_d.X_d + B.M + E.\delta_f - E_d.\delta_f \quad (28)$$

$$\dot{e} = A.e + B.M + (A - A_d).X_d + (E - E_d).\delta_f \quad (29)$$

The third part,  $(A - A_d).X_d$  and the fourth part  $(E - E_d).\delta_f$  in equation (29) can be treated as disturbance,  $W$  by the front wheel steering and the final equation becomes:

$$\dot{e} = A.e + B.M + W \quad (30)$$

#### A. Design of Linear Quadratic Regulator

Based on the optimal control theory in [19], an optimal control criterion can be archived by following this theory to any given system of control law. Using the optimal control theory, the desired value of sideslip angle is set to zero to avoid the SUV from spinning (as discussed in Section I). In this case, the desired value of yaw rate in equation (22) is taken into account. The DYC is implemented in a form of feedback compensator by using Linear Quadratic Regulator (LQR) controller.

The LQR algorithm is used to get an optimal feedback control gain of  $K_{bk}$  by minimizing the cost function of  $J$  as shown in the following equation:

$$J = \int_0^\infty (e^T.Q.e + u^T.R.u)dt \quad (31)$$

where,

$$e = x - x_{des} = \begin{bmatrix} \beta \\ \gamma \end{bmatrix} - \begin{bmatrix} \beta_{des} \\ \gamma_{des} \end{bmatrix} \quad Q = \begin{bmatrix} G_{fb1} & 0 \\ 0 & G_{fb2} \end{bmatrix}$$

$$R = r_{fb}$$

An  $e$ , represents an error or different value of the state variable between the measured and desired value.  $Q$  is the weighting factor of state, while  $R$  is the control variable. The quadratic form  $(e^T.Q.e)$  represents the deviation of the state  $e$  from the initial state and the term of  $(u^T.R.u)$  represents the “cost” of control. For the fast convergence of the error, the value of  $Q$  should be bigger than the value of  $R$ . The solution of solving the Riccati equation can be found in detailed in [20], the feedback gain of  $K_{bk}$  can be achieved and the corresponding yaw moment feedback is:

$$M = -K_{bk1}.(\beta - \beta_d) - K_{bk2}.(\gamma - \gamma_d) \quad (32)$$

#### B. Design of Linear Quadratic Integral

The Linear Quadratic Integral (LQI) controller is a variation of LQR controller where the control law is derived from solving the Riccati Equation in the LQR framework with added integral regulation of output variable. To design the Linear Quadratic Integrator, firstly equation (30) is differentiated to derive the following equation:

$$\ddot{e} = A.\dot{e} + B.\dot{M} + \dot{W} \quad (33)$$

Then the equation is expanded to (34) and the subsequent result is simplified into equation (35) as follows:

$$\frac{d}{dt} \begin{bmatrix} \dot{e} \\ e \end{bmatrix} = \begin{bmatrix} A & 0 \\ 1 & 0 \end{bmatrix} \begin{bmatrix} \dot{e} \\ e \end{bmatrix} + \begin{bmatrix} B \\ 0 \end{bmatrix} \dot{M} + Z \quad (34)$$

$$\dot{X}_r = A_r.X_r + B_r.\dot{M} + Z \quad (35)$$

where,

$$X_r = \begin{bmatrix} \dot{\beta} - \dot{\beta}_d \\ \dot{\gamma} - \dot{\gamma}_d \\ \beta - \beta_d \\ \gamma - \gamma_d \end{bmatrix} \quad A_r = \begin{bmatrix} \frac{C_f l_f}{mv_x^2} - 1 & \frac{C_f + k_r}{mv_x} & 0 & 0 \\ \frac{C_f l_f^2}{I_{zz} V_x} & \frac{C_f l_f + C_r l_r}{I_{zz}} & 0 & 0 \\ 1 & 1 & 0 & 0 \\ 1 & 1 & 0 & 0 \end{bmatrix}$$

$$B_r = \begin{bmatrix} 0 \\ \frac{1}{I_z} \\ 0 \\ 0 \end{bmatrix}$$

The disturbance of  $Z$  in equation (35) is equal to zero and based on the optimal control theory, the new state feedback is:

$$\dot{M} = - \begin{bmatrix} G_{fb1}.(\dot{\beta} - \dot{\beta}_d) + G_{fb2}.(\dot{\gamma} - \dot{\gamma}_d) + \dots \\ \dots + G_{fb3}.(\beta - \beta_d) + G_{fb4}.(\gamma - \gamma_d) \end{bmatrix} \quad (36)$$

The  $G_{fb}$  is the feedback gain where it is used to minimize

the quadratic cost function  $J$  as represented by the following equation:

$$J = \int_0^{\infty} (X_r^T \cdot Q \cdot X_r + \dot{M}^T \cdot R \cdot \dot{M}) dt \quad (37)$$

The matrix  $Q$  represents the weight of the state and the  $R$  is the control vectors represented as the following:

$$Q = \begin{bmatrix} G_{fb1} & 0 & 0 & 0 \\ 0 & G_{fb2} & 0 & 0 \\ 0 & 0 & G_{fb3} & 0 \\ 0 & 0 & 0 & G_{fb4} \end{bmatrix} \quad R = r_{fb}$$

And for fast convergence of the error, the value of  $Q$  should be bigger than the value of  $R$ .

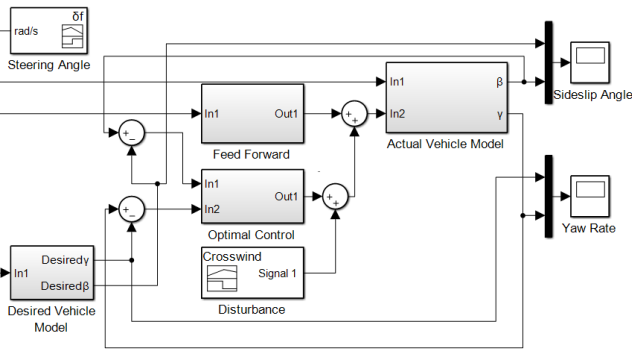


Figure 3: Block diagram of SUV system

#### IV. ANALYSIS AND RESULT

A computer simulation using MATLAB/Simulink has been conducted to study and evaluate the performance of the proposed controller. Figure 3 illustrates the full MATLAB /Simulink block model diagram system for the SUV and Table 1 shows the parameters of the SUV employed for the computer simulation analysis where the parameter was taken from [16].

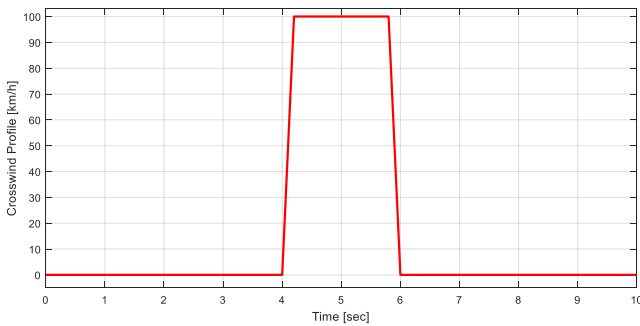


Figure 4: External disturbance crosswind [21]

For simulation analysis, the step steering manoeuvre was implemented to show how the reaction of SUV in two different conditions. The first condition was tested during dry road, which is the friction coefficient is 1.0 and the second condition was a wet road, where the friction coefficient is 0.5. As discussed in Section I, the design of the SUV has a drawback, in which the side area of the vehicle is bigger than the conventional vehicle, resulting in the vehicle to become more vulnerable to the crosswind effect. This subsequently leads to vehicle to be unstable and

loss control during this event. The external crosswind disturbances as shown in Figure 4 is added for both manoeuvres for the analysis of the performance of the controller.

Table 1  
Parameters of the SUV [16]

Symbol	Parameter (Unit)	Value
$m$	Mass (kg)	1592
$C_f$	Front Cornering Stiffness (N/rad)	-68420
$C_r$	Rear Cornering Stiffness(N/rad)	-68420
$H$	C.G Height (m)	0.72
$I_{zz}$	Yaw Inertia (kg.m <sup>2</sup> )	2488
$l_f$	Distance from C.G to front axle (m)	1.18
$l_r$	Distance from C.G to rear axle (m)	1.77
$v$	Vehicle Speed / Velocities (km/h)	100

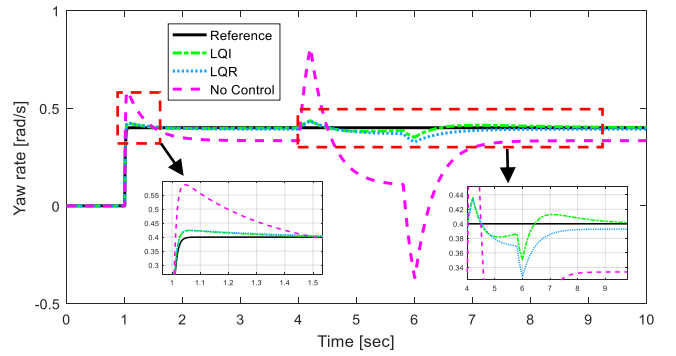


Figure 5: Step steering for yaw rate performance in 1.0μ

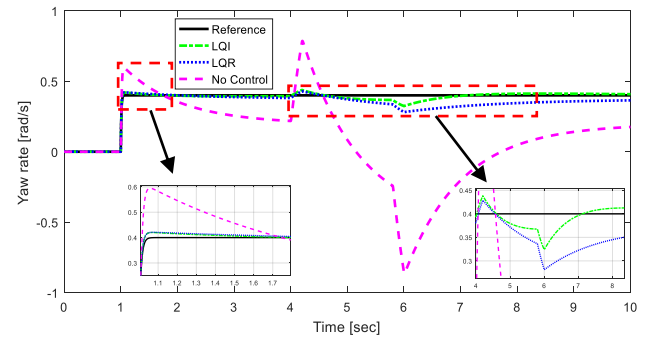


Figure 6: Step steering for yaw rate performance in 0.5μ

Figure 5 and 6 show the comparison of the road surface friction coefficient for  $\mu = 1.0$  (dry road) and 0.5 (wet road) for yaw rate, while Figure 7 and 8 is the comparison of sideslip angle. The step change started at  $t = 1s$  and the crosswind disturbance was added in a fixed time at  $t = 4s$  and ended at  $t = 6s$  with a wind speed of 100km/h. The simulation was carried out with an initial velocity of 100km/h.

In Figure 5, the result shows that the LQI has better tracking performance on the step steering test at  $t = 1s$ , where the LQI controller has minimum overshoot of 5.9% from the reference as compared with LQR, which has 6.1% overshoot. On the other hand, a vehicle without a controller has a maximum overshoot of 46.8% from the reference for yaw rate test. In this situation, the LQI and LQR controller can track the reference, except without the controller that has bigger overshoot and causes the SUV's stability loss.

As for the low friction coefficient ( $\mu = 0.5$ ) in Figure 6, the overshoot for LQI controller increased slightly to 7.3% and LQR controller also increased slightly to 7.9%, and



without a controller, it was 48.6% at  $t = 1$ s step steering. Since the friction is low, the LQI and LQR controller still can handle the manoeuvre without failing. As a system without a controller, obviously the SUV lost its controllability. Based on these results, both controllers can handle the step steering manoeuvre perfectly.

Table 2  
Response Index of Yaw Rate for Crosswind Disturbance

Yaw Rate	Dry Road ( $\mu = 1$ )		Wet Road ( $\mu = 0.5$ )	
	Max Peak [rad/s]	Settling Time[sec]	Max Peak [rad/s]	Settling Time[sec]
LQI	$3.509 \times 10^{-01}$	371	$3.240 \times 10^{-01}$	1.637
LQR	$3.272 \times 10^{-01}$	1.783	$2.831 \times 10^{-01}$	-
No Control	$-3.685 \times 10^{-01}$	-	$-8.635 \times 10^{-01}$	-

As for the response index for crosswind disturbance in Table 2, the LQI controller can overcome the disturbance much better than the LQR controller where the maximum peak is 12% compared to the LQR controller, which has 18.2% maximum peak from the reference. In the case of without controller, the maximum peak is 192% from a reference in the dry road. In this simulation, the settling time is  $\pm 5\%$  from the reference. The LQI controller is 79% respond faster for settling time compared to LQR controller. As for without controller, the settling time exceeded from the limit, as shown in Figure 5.

For the wet road, the LQI controller still can overcome the crosswind disturbance with 19% maximum peak from the reference compared with the LQR controller, which is 29% maximum peak from the reference. However, for the settling time, the LQR controller has exceeded from the acceptable limit, where the LQI controller still can track the desired yaw rate. As for without the controller, the vehicle motion cannot track the transient phase for a desired yaw rate as shown in Figure 6. The result demonstrates the superior effectiveness of the LQI controller in tracking performance compared with the LQR controller, when the external disturbance is injected into the system.

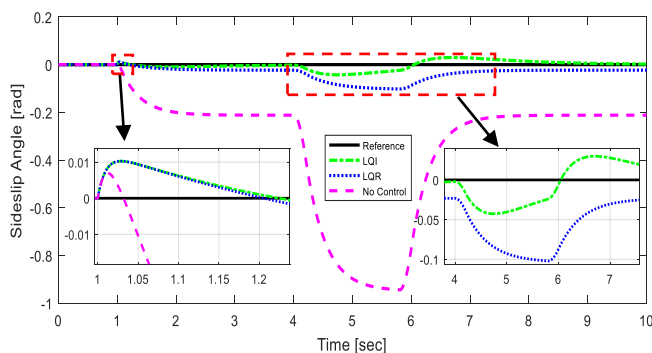


Figure 7: Step steering for sideslip performance for  $1.0\mu$

Figure 7 and Figure 8 show the result of sideslip angle for dry road and wet road respectively, and the response index for both simulations is shown in Table 3. The acceptable limit for sideslip angle is  $10^\circ$  or 0.175 rad. In Table 3, the LQI controller can restrain the vehicle sideslip angle in a narrow scope around 0.42% compared to LQR controller, which is 10.21%, although it is still in satisfactorily result. As for without the controller, the vehicle is spinning out of control or loss of stability because the vehicle has already exceeded the acceptable limit of sideslip angle at 94.4% of the dry road, as shown in Figure 7

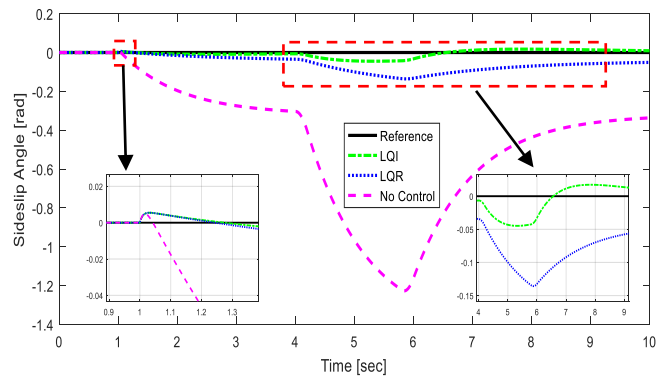


Figure 8: Step steering for sideslip performance for  $0.5\mu$

Table 3  
Response Index of Sideslip Angle

Sideslip Angle	Dry Road ( $\mu = 1.0$ )	Wet Road ( $\mu = 0.5$ )
	Max Peak [rad]	Max Peak [rad]
LQI	$-4.261 \times 10^{-02}$	$-4.476 \times 10^{-02}$
LQR	$-1.021 \times 10^{-01}$	$-1.358 \times 10^{-01}$
No Control	$-9.440 \times 10^{-01}$	-1.227

In the wet road condition, the LQI controller still can restrain the vehicle sideslip angle in the minimum peak of 0.48% compared with the LQR controller, which is 13.58%, although the LQR controller is still in acceptable limit. As for without the controller, the maximum peak, has increased to 122.7% and obviously, the vehicle is lost its stability, as shown in Figure 8. Considering these results, the LQI controller has a superior tracking performance compared with the LQR controller in the sideslip angle test.

## V. CONCLUSION

In this paper, an optimal yaw stability control for SUV is proposed and a validation method for DYC using Simulink/MATLAB simulation is presented. The crosswind disturbance is really affecting the stability and handling of SUV and the simulation result shows that the LQI controller is capable to overcome the disturbance much better than the LQR controller. As for system without the controller, the SUV obviously lost its controllability, especially when the disturbance is injected into the system in step steering manoeuvre test, as shown in this study.

## ACKNOWLEDGMENT

This work was supported by the Universiti Teknikal Malaysia Melaka (UTeM), Centre for Robotics and Industrial Automation and Ministry of Education (MOE) are greatly acknowledged. The research was funded by Research Acculturation Grant Scheme Grant No. (RAGS/1/2015/TK0/UTeM/03/18).

## REFERENCES

- [1] M. Fredette, L. S. Mambu, A. Chouinard, and F. Bellavance, "Safety impacts due to the incompatibility of SUVs, minivans, and pickup trucks in two-vehicle collisions," *Accid. Anal. Prev.*, vol. 40, no. 6, pp. 1987–1995, 2008.
- [2] N. Takubo and K. Mizuno, "Accident analysis of Sports Utility Vehicles: Human factors from statistical analysis and case studies," *JSAE Rev.*, vol. 21, no. 1, pp. 103–108, 2000.
- [3] D. Margaritis, B. Hoogvelt, Y. De Vries, C. Klootwijk, and H. Mooi, "An Analysis Of Sport Utility Vehicles Involved In Road Accidents," *ESV, Enhanc. Saf. Veh.*, no. 5, pp. 1–10, 2005.

- [4] S. S. Shadrin and A. M. Ivanov, "Algorithm of Autonomous Vehicle Steering System Control Law Estimation while the Desired Trajectory Driving," vol. 11, no. 15, pp. 9312–9316, 2016.
- [5] M. Z. Azmi et al., "Steering intervention strategy for side lane collision Avoidance," *ARPJ. Eng. Appl. Sci.*, vol. 12, no. 14, pp. 4265–4269, 2017.
- [6] F. Liu, L. Xiong, and X. Wu, "Design and Experimental Validation for Stability Control of Four-Wheel-Drive Electric Vehicle," in *IEEE Conference and Expo Transportation Electrification Asia-Pacific (ITEC Asia-Pacific)*, 2014, pp. 1–4.
- [7] S. Zhu and Y. He, "Design of SUV differential braking controller considering the interactions of driver and control system," in *Proceedings of the ASME 2014 International Mechanical Engineering Congress and Exposition*, 2014, pp. 14–20.
- [8] H. Dengbo, L. Hui, and Y. Fan, "Study on Vehicle Stability Control by Using Model Predictive Controller and Tire-road Force Robust Optimal Allocation," *SAE Int. J. Commer. Veh.*, vol. 8, no. 1, pp. 126–136, 2015.
- [9] A. Elhefnawy, A. . Sharaf, H. . Ragheb, and S. Hegazy, "Active Vehicle Safety using Integrated Control of Body Roll and Direct Yaw Moment," in *Proceedings of the 17th Int. AMME Conference*, 2016, no. April, p. 17.
- [10] V. Muniandy, P. M. Samin, and H. Jamaluddin, "Application of a self-tuning fuzzy PI–PD controller in an active anti-roll bar system for a passenger car," *Veh. Syst. Dyn.*, vol. 53, no. 11, pp. 1641–1666, 2015.
- [11] B. DO Anderson and J. B. Moore, *Optimal control: linear quadratic methods*. Courier Corporation, 2007.
- [12] J. HAN, Y. PARK, and Y. PARK, "Cooperative Regenerative Braking Control For Front- Wheel-Drive Hybrid Electric Vehicle Based On Adaptive Regenerative Brake Torque Optimization Using Under-Steer Index," *Int. J. Automot. Technol.*, vol. 15, no. 6, pp. 989–1000, 2014.
- [13] S. Yim, "Design of a robust controller for rollover prevention with active suspension and differential braking," *J. Mech. Sci. Technol.*, vol. 26, no. 1, pp. 213–222, 2012.
- [14] Z. Jin, C. Wang, L. Zhang, and A. Khajepour, "Multi-objective cooperative control of vehicle stability with electro hydraulic brake," in *Advanced Vehicle Control: Proceedings of the 13th International Symposium on Advanced Vehicle Control*, 2016, p. 235.
- [15] L. Song and Y. He, "The Design of SUV Anti Rollover Controller Based on Driver-in-the-Loop Real-Time Simulations," in *International Conference on Intelligent Computing*, 2016, pp. 509–519.
- [16] X. Ding and Y. He, "Application of driver-in-the-loop real-time simulations to the design of SUV differential braking controllers," *Intell. Robot. Appl.*, vol. 7506 LNAI, pp. 121–131, 2012.
- [17] H. G. Malkapure and M. Chidambaram, "Comparison of Two Methods of Incorporating an Integral Action in Linear Quadratic Regulator," in *IFAC Proceedings Volumes*, 2014, vol. 47, pp. 55–61.
- [18] R. Rajamani, *Vehicle Dynamics and Control*, Second edi. Boston, MA: Springer US, 2012.
- [19] B. D. O. Anderson and J. B. Moore, *Optimal control: Linear Quadratic Methods*. Prentice-Hall Inc., London, UK, 1990.
- [20] A. E. Bryson, *Applied optimal control: optimization, estimation and control*, Second edi. CRC Press, 1975.
- [21] N. M. Ghani, Y. M. Sam, and A. Ahmad, "Active steering for vehicle system using sliding mode control," in *Research and Development*, 2006. SCORed 2006., 2006, pp. 256–261.
- [22] M. Shino, N. Miyamoto, Y.-Q. Wang, and M. Nagai, "Traction control of electric vehicles considering vehicle stability," *6th Int. Work. Adv. Motion Control Proc.*, pp. 311–316, 2000.